Oyster larval transport in coastal Alabama: Dominance of physical transport over biological behavior in a shallow estuary

Choong-Ki Kim,[1] Kyeong Park,[2] Sean P. Powers,[2] William M. Graham,[2] and Keith M. Bayha[2]

Received 15 January 2010; revised 29 April 2010; accepted 5 May 2010; published 8 October 2010.

[1] Among the various factors affecting recruitment of marine invertebrates and fish, larval transport may produce spatial and temporal patterns of abundance that are important determinants of management strategies. Here we conducted a field and modeling study to investigate the larval transport of eastern oyster, *Crassostrea virginica*, in Mobile Bay and eastern Mississippi Sound, Alabama. A three-dimensional larval transport model accounting for physical transport, biological movement of larvae, and site- and larval-specific conditions was developed. A hydrodynamic model was used to simulate physical transport, and biological movement was parameterized as a function of swimming and sinking velocity of oyster larvae. Site- and larval-specific conditions, including spawning location, spawning stock size, spawning time, and larval period, were determined based on the previous studies. The model reasonably reproduced the observed gradient in oyster spat settlement and bivalve larval concentration, although the model results were less dynamic than the data, probably owing to the simplified biological conditions employed in the model. A persistent gradient decreasing from west to east in the model results at time scales of overall average, season, and each survey in 2006 suggests that the larval supply may be responsible for the corresponding gradient in oyster spat settlement observed over the past 40 years. Biological movement increased larval retention near the spawning area, thus providing a favorable condition for local recruitment of oysters. Inclusion of biological movement, however, caused little change in the overall patterns of larval transport and still resulted in a west-east gradient, presumably because of frequent destratification in the shallow Mobile Bay system.

Citation: Kim, C.-K., K. Park, S. P. Powers, W. M. Graham, and K. M. Bayha (2010), Oyster larval transport in coastal Alabama: Dominance of physical transport over biological behavior in a shallow estuary, *J. Geophys. Res.*, *115*, C10019, doi:10.1029/2010JC006115.

1. Introduction

[2] Persistence of exploitable populations of marine invertebrates and fish is dependent on a high influx of new recruits into a population. For most marine invertebrates and fish this influx occurs during the planktonic larval stage and is a function of both concentrations of larvae in the water column and horizontal advection into the region, that is, larval supply [*Yund et al.*, 1991]. Larval supply is influenced by a combination of physical transport and biological movement of larvae [*Morgan*, 1995; *Kennedy*, 1996]. Physical transport, defined as larval transport not affected by larval characteristics but solely determined by physical processes, includes advection and turbulent mixing. Physical transport processes that enhance larval retention play a critical role in successful recruitment of larval organisms within outflux-dominant estuaries [*Andrews*, 1983]. In the James River estuary, horizontal and vertical circulation and turbulent mixing associated with a frontal system combine to enhance upstream transport of oyster larvae and, thus, contribute to larval retention [*Andrews*, 1983; *Mann*, 1988; *Shen et al.*, 1999]. *Andrews* [1983] suggested that the ultimate fate of bivalve larvae is strongly dependent on current regimes and flushing rates of estuaries. Similarly, tidal currents, wind-driven circulation, and gravitational circulation promote transport of blue crab larvae into estuarine nursery areas and enhance their retention near settling areas in the northern Gulf of Mexico [*Rabalais et al.*, 1995; *Morgan et al.*, 1996; *Perry et al.*, 2003].

[3] Biological movement, defined as larval movement in the vertical direction influenced by larval characteristics such as larval size, density, and behavior, includes sinking and swimming of larvae, that is, all vertical transport except that due to vertical advection and turbulent mixing. Biological movement of larvae has been suggested to explain observed patterns of oyster larval distribution in several

[1]Department of Biology, Stanford University, Stanford, California, USA.
[2]Department of Marine Sciences, University of South Alabama, Dauphin Island Sea Lab, Dauphin Island, Alabama, USA.

0148-0227/10/2010JC006115

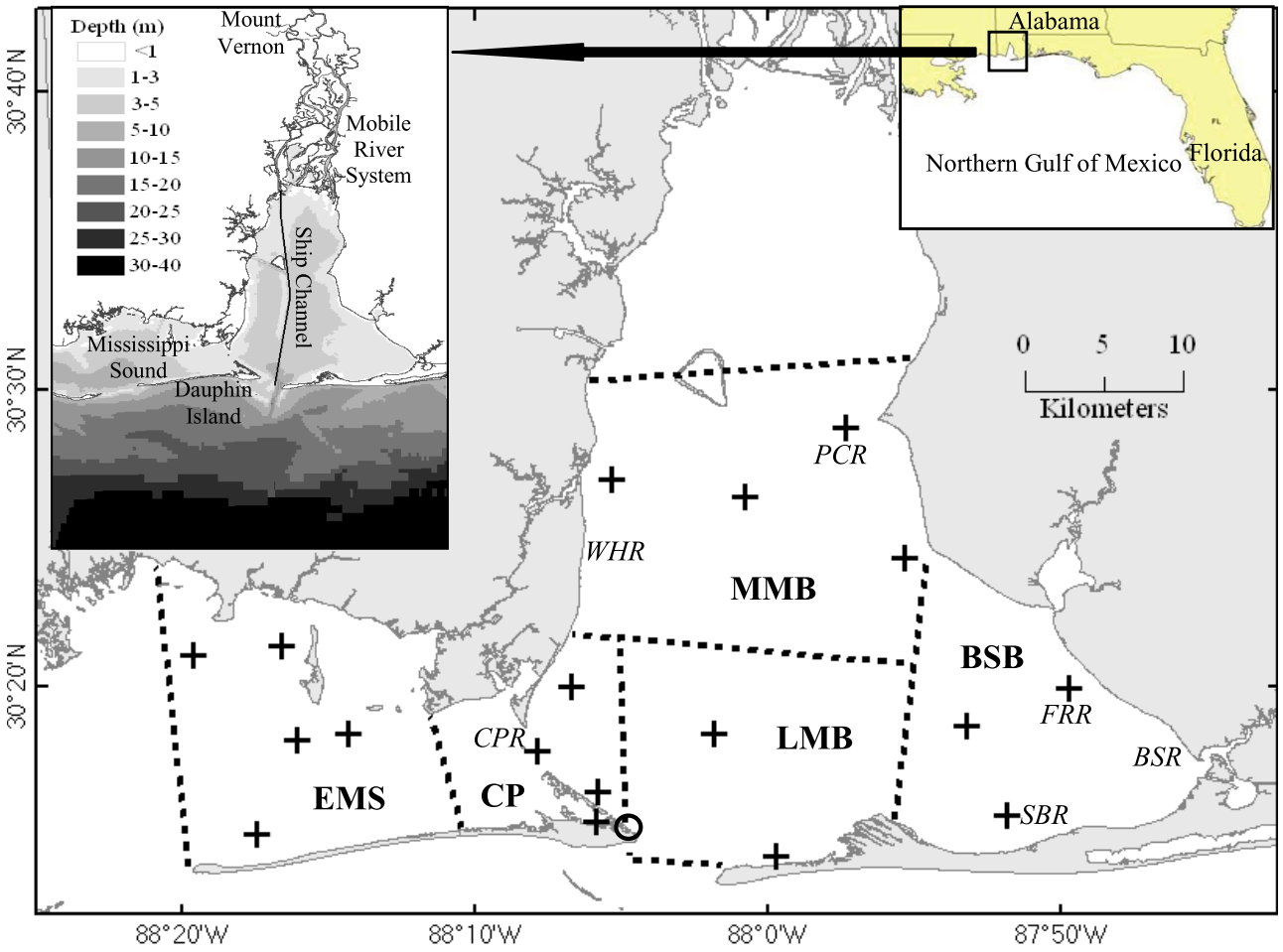

Figure 1. A map of Mobile Bay and adjacent eastern Mississippi Sound showing 18 mooring stations (crosses), Dauphin Island/Dauphin Island Sea Lab (DISL) station (open circle), and six existing oyster reefs, where oyster larvae were released in model simulations: Cedar Point Reef (CPR), White House Reef (WHR), Point Clear Reef (PCR), Fish River Reef (FRR), Bon Secour Reef (BSR), and Shell Bank Reef (SBR). Dashed lines denote boundaries of five zones: Eastern Mississippi Sound (EMS), Cedar Point (CP), Lower Mobile Bay (LMB), Middle Mobile Bay (MMB), and Bon Secour Bay (BSB). The map in the top left corner shows the modeling domain with depth contours.

estuaries. In New Jersey estuaries and Prince Edward Island, Canada, differential vertical distributions of oyster larvae were observed in relation to variations in biological movement with tidal phases and stratification [*Carriker*, 1951; *Kennedy*, 1996]. In estuaries of New Jersey [*Carriker*, 1951] and James River [*Andrews*, 1983], early-stage oyster larvae were randomly distributed throughout the water column and late-stage larvae were found frequently near the bottom. These distributions suggested that biological movement may play an important role in vertical positioning and the subsequent upstream transport of late-stage larvae. *North et al.* [2008] found that differences in biological movement of oyster larvae had greater influence on spatial patterns of larval transport than did interannual differences in circulation patterns in Chesapeake Bay. In contrast, earlier studies (see review by *Korringa* [1952]) found no evidence of biological movement for upstream transport of late-stage oyster larvae and that physical transport of larvae is the dominant factor. *Andrews* [1983], despite observations of continuous swimming of oyster larvae, concluded that physical transport dominates over biological movement. Despite these controversial arguments about the role of biological movement, the interaction between physical transport and biological movement has been suggested as the primary explanation for unidirectional horizontal transport or retention of invertebrate larvae in estuarine systems [*Wood and Hargis*, 1971; *Andrews*, 1983; *Rothlisberg et al.*, 1983; *Mann*, 1988; *Morgan et al.*, 1996; *North et al.*, 2008].

[4] Mobile Bay is a broad, shallow (average depth of 3 m) estuary with a narrow (120 m) and deep (12–14 m) ship channel located in the northern Gulf of Mexico (Figure 1). Hydrodynamic conditions in Mobile Bay and eastern Mississippi Sound are influenced by tide, river discharge, and wind, with their relative impacts varying spatially and temporally [*Wiseman et al.*, 1988; *Schroeder et al.*, 1990; *Noble et al.*, 1996; *Ryan et al.*, 1997]. Observations in Mobile Bay and eastern Mississippi Sound, Alabama, showed a persistent gradient decreasing from west to east in oyster spat settlement over the past 40 years: significant settlement in the southwest side of Mobile Bay and eastern Mississippi

Table 1. Times and Other Conditions of Field Surveys in 2006

Survey ID	Survey Dates	Average Water Temperature[a] (°C)	Larval Period[b] (days)	Spawning Time[c]
11	16-22 May	24.7	14	1600 on 2 May
12	07–08 Jun	28.3	11	1500 on 25 May
13	27–29 Jun	29.4	10	1700 on 16 Jun
14	17–19 Jul	30.2	10	0800 on 7 Jul
15	07–09 Aug	30.4	10	1400 on 28 Jul
16	29–30 Aug	31.2	10	1400 on 16 Aug
17	20–21 Sep	29.3	10	0900 on 7 Sep
18	09–11 Oct	26.8	12	1000 on 25 Sep
19	30–31 Oct	22.0	18	0500 on 14 Oct

[a]Average bottom water temperature over the time period since the previous survey, calculated from the hourly data at the Dauphin Island Sea Lab station (Figure 1).
[b]Larval period estimated using equation (5).
[c]An increase in bottom-water temperature to a critical threshold of 25°C was used to detect the initial spring spawning for survey 11, and a rapid change over 2°C was used for the summer and fall spawning for surveys 12 to 19.

Sound and negligible settlement in the middle and east side of the Bay [*Hoese et al.*, 1972; *Lee*, 1979; *Saoud et al.*, 2000]. *Hoese et al.* [1972] attributed the lower spat settlement in the east side of the Bay to the relatively low larval supply. *Saoud et al.* [2000] suggested that different larval and water sources, controlled by different flow patterns, may be responsible for different peaks in larval supply, thus resulting in spatially different settlement intensity. Although the characteristics of larval transport have been inferred from spat settlement data, no direct studies have been conducted on oyster larval transport in the Mobile Bay system, and little is known about the controlling processes responsible for the persistent west-to-east gradient in oyster spat settlement.

[5] We conducted a field and modeling study to investigate the larval transport, supply, and settlement of eastern oyster (*Crassostrea virginica*) in Mobile Bay and eastern Mississippi Sound, Alabama. Data for oyster spat settlement and bivalve larval concentration were collected in 2006 to examine spatial and temporal distribution patterns. A three-dimensional larval transport model accounting for both physical transport and biological movement of oyster larvae was developed. The model results, with or without biological movement, were compared with data for oyster spat settlement and bivalve larval concentration. Model sensitivity was examined for the parameterization of biological movement, spawning time, and larval period. The larval transport model was used to investigate the characteristics of oyster larval transport in the Mobile Bay system with specific reference to the following questions: (1) Is larval transport responsible for the persistent gradient in oyster spat settlement decreasing from west to east observed over the past 40 years? (2) Are there seasonal variations in larval transport and retention? and (3) How does biological movement of oyster larvae influence their transport?

2. Materials and Methods

2.1. Field Data

[6] Two types of field data, spat settlement of oysters and larval concentration of bivalves, were collected at 18 mooring stations in Mobile Bay and eastern Mississippi Sound (Figure 1). Seven stations were located near existing oyster reefs, including Cedar Point Reef (CPR), White House Reef (WHR), Point Clear Reef (PCR), Fish River Reef (FRR), Bon Secour Reef (BSR), and Shell Bank Reef (SBR), with 11 additional stations located throughout the mesohaline portions of the study area. The field survey was conducted every 3 weeks from January to December in 2006, with CTD casting to collect water column information using a Sea-Bird profiler (SBE25).

[7] Spat settlement was measured using regular deployment of collection tiles. Two PVC circular panels 25 cm in diameter attached to a stainless-steel pipe anchored to a concrete mooring at each station. Both PVC panels were placed perpendicular to the mooring so that the plates rested in a horizontal position. Three settlement plates made by 12 × 12 cm cement board, similar to those used by *Hoese et al.* [1972], were placed on both upper and lower PVC panels attached 1.0 and 0.5 m from the bottom, respectively. One of the plates (covered plate) was enclosed with a 4 mm mesh plastic cage and the second plate (partially covered plate) had a partial cage with two sides open, that is, the top and two sides were enclosed, while the third plate (uncovered plate) was not modified. The covered plates were intended to measure oyster spat settlement in the absence of predation by excluding oyster drills and crabs from the cage. The uncovered plates allowed assessment of spat settlement in the presence of predators. The partially covered plates baffled water flow but allowed predator access, thus allowing assessment of hydrodynamic artifacts of caging on oyster spat settlement.

[8] Settlement plates were retrieved and replaced with new plates every 3 weeks. The plates were placed on ice following retrieval and then frozen at the lab until analysis. The total number of oyster spats on each plate was counted using microscopy. Covered plates were expected *a priori* to show the highest oyster spat settlement because predators were excluded; however, the highest settlement was normally observed in partially covered plates, suggesting that cage treatments did not work well. Maximum oyster spat settlement among three treatments was selected from each of the upper and lower panels as the best representation of the larval supply of oysters at each station, and their average was used for subsequent analysis. Although the field program was conducted from January to December in 2006, only the data from nine surveys, surveys 11 to 19, in May–October, when mass spat settlement (i.e., maximum settlement reaches up to 97–563 spat m^{-2} day^{-1}) occurred, are discussed in this paper. The times and other conditions of the surveys are reported in Table 1.

[9] During each spat settlement survey, bivalve larvae were sampled at 18 stations by collecting 10 L of seawater via pump (Rule Model 3700) from 0.5 m above the bottom and passing this water through a 35 μm mesh plankton net (Sea-Gear Corp., Melbourne, FL). The particles trapped in the net were immediately separated using a sieve array consisting of 500, 100, and 30 μm mesh screens. The resulting two size classes of particles, 30–150 and 150–500 μm (after allowing for diagonal length of screen mesh), were split via plankton splitter, and one-fourth of the total samples were preserved in 4% buffered formaldehyde for microscopic analysis. Since microscopic identification of bivalve larvae

at these sizes is extremely difficult [*Carriker*, 1996], all bivalve larvae including oyster larvae were counted using microscopy. We used the data for the size class of 150–500 μm as a measure of late-stage larval concentration.

[10] Both data for oyster spat settlement and bivalve larval concentration were $\log_{10}$ transformed due to variance exceeding means. To examine spatial differences, 18 stations were grouped into five zones based on the collected data and existing oyster reefs (Figure 1): eastern Mississippi Sound (EMS; n = 5), Cedar Point (CP; n = 4), lower Mobile Bay (LMB; n = 2), middle Mobile Bay (MMB; n = 4), and Bon Secour Bay (BSB; n = 3). To examine seasonal variations, nine surveys were grouped into three seasons: spring (surveys 11–13), summer (surveys 14–16), and fall (surveys 17–19). Average water temperature varied from 24.7° to 29.4°C, from 30.2° to 31.2°C, and from 22.0° to 29.3°C in spring, summer, and fall, respectively (Table 1). Seasonal patterns were also observed in salinity. Average salinity at the surface (bottom) was 18.0 psu (21.1 psu), 24.0 psu (25.3 psu), and 23.1 psu (24.3 psu) in spring, summer, and fall, respectively, representing the largest freshwater discharge in spring and the lowest in summer. Salinity, however, showed great spatial variability, for example, ranging from 3.0 to 31.3 psu in survey 11. One-way analysis of variance (ANOVA) was conducted to examine differences between zones with five levels. If ANOVA indicated significant differences between zones at $p < 0.05$, Tukey multiple-comparison tests were conducted to determine which zones were significantly different. Correlation analysis was conducted to investigate the relationship between spat settlement and larval concentration. All statistical tests were conducted in MINITAB V14.2.

2.2. Larval Transport Model

[11] The governing mass-balance equation for oyster larvae in Cartesian coordinates may be expressed as

$$\frac{\partial C}{\partial t} = -\frac{\partial (uC)}{\partial x} - \frac{\partial (vC)}{\partial y} - \frac{\partial (wC)}{\partial z} + \frac{\partial}{\partial x}\left(K_x \frac{\partial C}{\partial x}\right) + \frac{\partial}{\partial y}\left(K_y \frac{\partial C}{\partial y}\right) + \frac{\partial}{\partial z}\left(K_z \frac{\partial C}{\partial z}\right) - w_{\mathrm{bi}} \frac{\partial C}{\partial z}, \quad (1)$$

where t is time; x, y, and z are the east, north, and vertical coordinates, respectively; C is the larval concentration; u, v, and w are the current velocity components in the x, y, and z directions, respectively; K_x, K_y, and K_z are the turbulent diffusivities in the x, y, and z directions, respectively; and w_{bi} is the net vertical velocity for biological movement of larvae. The first term in equation (1) indicates the time rate change in larval concentration. The first three terms on the right-hand side represent advective transport and the next three terms represent turbulent diffusive transport, which combine to determine physical transport of larvae and are independent of a target organism. The last term indicates net biological movement of larvae, which varies as a function of larval characteristics such as larval size, density, and behavior, that is, all vertical transport except that due to vertical advection and turbulent mixing. Horizontal movement of oyster larvae is not considered because most small larvae cannot swim fast enough in a horizontal direction to influence their distribution over a strong horizontal velocity of physical transport [*Young*, 1995].

2.2.1. Physical Transport

[12] The hydrodynamic model in the three-dimensional hydrodynamic-eutrophication model (HEM3D), also referred to as the environmental fluid dynamics code (EFDC), was applied to simulate physical transport of oyster larvae. The model is based on turbulence-averaged governing equations, including continuity, momentum, salt-balance, and heat-balance equations, with hydrostatic and Boussinesq approximations [*Hamrick*, 1992]. Because the spatial density gradient is virtually determined by the salinity gradient in the study area (see section 3.1.1), the present model application did not solve the heat-balance equation and calculated density as a function of salinity only. For turbulence closure, the model employs the second moment turbulence model developed by *Mellor and Yamada* [1982] and modified by *Galperin et al.* [1988]. The model has been successfully applied to a number of systems [*Ji et al.*, 2001; *Lin and Kuo*, 2003], and a more detailed description of the model is given by *Hamrick* [1992, 1996].

[13] The modeling domain (88°30.18′–87°41.35′W, 29°50.70′–31°05.03′N) includes Mobile Bay, the Mobile River system, eastern Mississippi Sound, and the northern Gulf of Mexico (Figure 1). The seaward open boundary was extended southward to about 45 km south of Dauphin Island and the upriver boundary was at Mount Vernon. An orthogonal curvilinear grid was used to resolve the complex shoreline and bottom topography. The grid system has 21,705 surface water cells and five vertical σ layers, with the grid size varying from 58 to 2000 m. The finest grid cells are small enough to resolve the narrow ship channel and to allow us to turn off horizontal eddy diffusion.

[14] The model became stabilized within a few tidal cycles with arbitrary (0) initial conditions for surface elevation and velocity, that is, cold start. To estimate the initial condition for salinity, an ideal model run was conducted, forced by harmonic tide with the two most important constituents (K1 + O1), 31 year (1976–2006) median river discharge, and 20 year (1987–2006) median wind speed and random wind direction. The tidal average salinity field calculated after the ideal model run reached steady state was used for the initial salinity condition, which was specified after 5 days of initial warming-up of cold start. The model application gave a good reproduction of the observed surface elevation, current velocity, and salinity for both total and subtidal components and was able to simulate the features observed to be important for mass transport in the Mobile Bay system; see [*Kim*, 2009].

2.2.2. Biological Movement of Oyster Larvae

[15] Net biological movement of oyster larvae was parameterized as a function of swimming and sinking velocity, which varies with larval size.

2.2.2.1. Larval Size

[16] Larval swimming and sinking velocity varies as larvae grow. Fertilized eggs develop into trochophores in 6–9 h, and these develop into veligers in 24–48 h [*Galtsoff*, 1964; *Burrell*, 1986; *Carriker*, 1996]. After a 10–20 day larval period, veligers develop into pediveligers with a foot. Pediveligers tend to stay near bottom and can crawl short distances to find suitable substrates for settlement. If suitable substrates are found, pediveligers permanently settle on the substrates and metamorphose into oyster spats for the benthic life cycle. Larval size, about 40–60 μm for trocho-

phores, increases as they develop and settlement occurs when the larval size is between 300 and 350 μm [*Galtsoff*, 1964; *Carriker*, 1996; *Kennedy*, 1996]. The maximum larval size for the late-stage larvae varies depending on environmental conditions such as food availability, temperature, salinity, dissolved oxygen (DO), and turbidity [*Dekshenieks et al.*, 1993; *Kennedy*, 1996]. Because the maximum larval size tends to be smaller in southern than northern latitudes [*Kennedy*, 1996], the lower limit of maximum larval size, 300 μm, may be a better representative of oyster larvae in the Gulf of Mexico. In this study, oyster larval size is assumed to increase linearly from 50 to 300 μm during a larval period.

2.2.2.2. Swimming Velocity

[17] Swimming velocity represents the processes contributing to the retention of larvae in the water column and may be influenced by many processes including larval size, temperature, salinity and salinity gradient, DO, gravity, light, and chemical cues [*Hidu and Haskin*, 1978; *Mann and Rainer*, 1990; *Mann et al.*, 1991; *Turner et al.*, 1994; *Young*, 1995; *Dekshenieks et al.*, 1996; *Kennedy*, 1996; *Dekshenieks et al.*, 1997]. Although there is no consensus on what stimulates larval swimming behavior, the observed swimming velocity, despite the differences in experimental conditions, generally increases from 0.4 to 3.1 mm s^{-1} as oyster larvae grow.

[18] In the present study swimming velocity was parameterized as a function of larval size by employing a linear regression based on the data for eastern oyster larvae by *Hidu and Haskin* [1978, Figure 2], *Mann* [1988, Table 5], and *Mann and Rainer* [1990, Table 1]:

$$w_{\mathrm{swim}} = 0.0089L - 0.0076, \tag{2}$$

where w_{swim} is the swimming velocity (mm s^{-1}) and L is the larval length (μm). The linear regression shows a significant relationship between w_{swim} and larval size ($R^2 = 0.74$, $p < 0.001$; $n = 13$), and the estimated w_{swim} increases from 0.4 to 2.7 mm s^{-1} as larvae grow from 50 to 300 μm, comparable with the estimates of *Dekshenieks et al.* [1996], ranging from 0.0 to 2.4 mm s^{-1}.

2.2.2.3. Sinking Velocity

[19] Sinking velocity indicates the downward velocity of larvae and varies as a function of larval size. As larvae grow their size increases, their shells become thicker and heavier, and the mass-to-area ratio increases, thus resulting in an increased density and sinking velocity [*Galtsoff*, 1964; *Mann et al.*, 1991; *Dekshenieks et al.*, 1997; *Baker and Mann*, 2003]. *Hidu and Haskin* [1978] observed that the sinking velocity of eastern oyster larvae varied little for different salinities, but increased from 0.7 to 8.3 mm s^{-1} with increasing larval size. They suggested that sinking velocity could dominate over swimming velocity during the late stage of larvae, which can be advantageous for pediveliger larvae.

[20] Empirical formulations have been proposed for sinking velocity. *Mann et al.* [1991] expressed the sinking velocity of bivalve larvae including oyster larvae as a linear or square function of larval size. *Dekshenieks et al.* [1996] parameterized sinking velocity with an exponential function of larval size. These empirical equations all indicate a positive relationship between sinking velocity and larval size, but with different rates of increase in sinking velocity with larval growth.

[21] In the present study sinking velocity was parameterized as a function of larval size by employing a linear regression based on the data for eastern oyster larvae of *Hidu and Haskin* [1978, Figure 3]:

$$w_{\mathrm{sink}} = 0.0304L - 1.099, \tag{3}$$

where w_{sink} is the sinking velocity (mm s^{-1}). The linear regression shows a significant relationship between w_{sink} and larval size ($R^2 = 0.98$, $p < 0.001$; $n = 20$), and the estimated w_{sink} increases from 0.4 to 8.0 mm s^{-1} as larvae grow from 50 to 300 μm, comparable with the estimates of *Mann et al.* [1991], ranging from 0.0 to 8.2 mm s^{-1}.

2.2.2.4. Net Vertical Velocity

[22] Many studies have considered biological movement of bivalve larvae determined by a combination of swimming and sinking behavior [*Jonsson et al.*, 1991; *Dekshenieks et al.*, 1996; *Wang and Xu*, 1997]. Although it is still not clear how to combine the two opposing processes at various stages of oyster larvae, a consensus based on observations does exist concerning the vertical distribution of oyster larvae. Oyster larvae tend to stay in the water column at the early stage, often showing peaks near the pycnocline, but accumulate in the bottom layer for settlement at late stages [*Carriker*, 1951; *Andrews*, 1983; *Mann*, 1988; *Dekshenieks et al.*, 1996; *Kennedy*, 1996]. For early-stage larvae ranging between 50 and 150 μm, the sinking velocity varies from 0.4 to 3.5 mm s^{-1} (equation (3)). That is, sinking behavior alone would make them reach the bottom in 0.8–6.9 h for a water depth of 10 m. Early-stage larvae then should show swimming behavior so that net biological movement is either neutrally buoyant or even upward, for them to stay in the water column. For late-stage larvae, in contrast, sinking behavior should dominate over swimming behavior so that net biological movement is downward sinking to accumulate them in the bottom layer.

[23] *Dekshenieks et al.* [1996] expressed the net vertical velocity of oyster larvae as a function of swimming and sinking velocity using the concept of percentage time swimming:

$$w_{\mathrm{bi}} = \mathrm{TS}\,w_{\mathrm{swim}} - (1 - \mathrm{TS})\,w_{\mathrm{sink}}, \tag{4}$$

where w_{bi} is the net vertical velocity of oyster larvae (mm s^{-1}), and TS is the percentage time spent swimming by larvae. *Dekshenieks et al.* [1996] expressed TS as a function of salinity change and estimated it to vary from 64% to 83% for a typical salinity variation within a tidal cycle. Using TS = 74% (middle of the reported range), with the present parameterization methods of swimming (equation (2)) and sinking (equation (3)) velocity, equation (4) gives reasonable estimates of w_{bi} in light of the basic premise: net upward movement of early-stage larvae and net downward movement of late-stage larvae (crosses in Figure 2). *Dekshenieks et al.* [1996], using equation (4), simulated the vertical distribution of oyster larvae in a vertical one-dimensional model and compared the model results with the data of *Carriker* [1951]. Their model results for early-stage larvae show the peak larval concentration in the surface layer, while the observed peak was near mid depth [*Dekshenieks et al.*, 1996, Figure 6], suggesting that equation (4) may

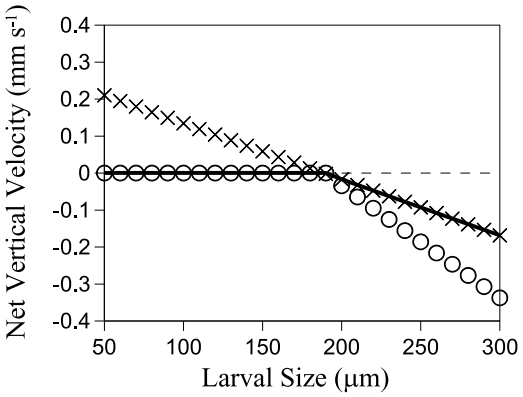

Figure 2. Net vertical velocity as a function of oyster larval size. VM (bold solid line) is for neutral buoyancy at the early stage and net sinking at the late stage, VM_{swim} (crosses) is for net swimming at the early stage and net sinking at the late stage, and VM_{sink} (open circles) is for neutral buoyancy at the early stage and twice-as-fast net sinking at the late stage.

overestimate net upward swimming for early-stage oyster larvae. For late-stage larvae both the model results and the data show peak concentration near the bottom.

[24] The present model employs neutrally buoyant net vertical velocity ($w_{bi} = 0$) for early-stage larvae from 50 to 190 μm and net sinking velocity for late-stage larvae from 190 to 300 μm (VM in Figure 2). For the latter the model uses w_{bi} estimated using equation (4). The model sensitivity was examined for net swimming of early-stage larvae (VM_{swim} in Figure 2) and twice-as-fast net sinking of late-stage larvae (VM_{sink} in Figure 2).

2.3. Model Setup

2.3.1. Forcing Functions

[25] Surface elevation, river discharge, and wind conditions were specified as forcing functions. Hourly surface elevation data at the National Oceanic and Atmospheric Administration (NOAA)'s Dauphin Island station (Figure 1) were used to specify the open boundary condition after being adjusted for amplitude and phase as described by *Kim* [2009]. Daily river discharge during the larval period for each survey shows that discharge greater than 4500 $m^3\ s^{-1}$ occurred for survey 11 and that relatively low and constant discharge, less than 500 $m^3\ s^{-1}$, prevailed for surveys 12 to 18 (Figure 3). Moderate river discharge, up to 1200 $m^3\ s^{-1}$, occurred for survey 19. Hourly wind data, observed at the Dauphin Island station by the National Data Buoy Center (NDBC), show a seasonal pattern. In spring (surveys 11–13) and summer (surveys 14–16), south winds were dominant. In fall (surveys 17–19) north winds became dominant, with a stronger speed.

2.3.2. Site- and Larval-Specific Conditions

[26] Conditions for spawning location, spawning time, spawning stock size, and larval period are required for larval transport simulations. Spawning location and time are needed to determine where and when to release larvae, spawning stock size determines how many larvae to be released, and larval period defines how long to simulate larval transport. These conditions vary with site- and larval-specific biological and environmental conditions of a target estuary [*Dekshenieks et al.*, 1996; *Kennedy*, 1996; *Shumway*, 1996; *Thompson et al.*, 1996].

2.3.2.1. Spawning Location and Stock Size

[27] Oysters tend to aggregate and form biogenic reefs in an estuarine system. *Moore* [1913], *Bell* [1952], and *May* [1971] conducted intensive surveys of oyster reefs throughout Mobile Bay and eastern Mississippi Sound, and *Smith* [1999] observed the oyster density in Mobile Bay. These observations suggested that a consistent pattern, significantly higher oyster production in the southwestern part of the study area than the middle and east side, has existed for the past 90 years. Especially, CPR, located at the intersection of Mobile Bay and eastern Mississippi Sound, has been the most productive reef area, contributing over 90% of the oyster harvest in Alabama [*May*, 1971]. *Smith* [1999] found a significantly higher oyster density in CPR than in unproductive oyster reefs such as WHR, FRR, and SBR. Existing oyster reefs were considered as potential spawning locations and the present study assumed that oyster larvae were released at six live oyster reefs: CPR, WHR, PCR, BSR, FRR, and SBR (Figure 1).

[28] Reproduction of oysters varies depending on the characteristics of oysters, for example, oyster size, health, and nutrient reserves, as well as environmental conditions, for example, temperature, DO, turbidity, food availability, and latitude [*Thompson et al.*, 1996]. Oysters may spawn multiple times during reproduction periods and their fecundity may change in time [*Thompson et al.*, 1996]. Therefore, it is hard to determine the absolute spawning stock size for each spawning event from an oyster reef. Instead, we may estimate the relative spawning stock size based on the number of adult oysters in oyster reefs. The size of an oyster reef and oyster density may be good indicators to estimate the potential spawning stock size of a reef. In the present study we used current oyster harvest information, which states that the most productive oyster reefs (CPR) contribute over 90% of the oyster harvest in Alabama [*May*, 1971], to estimate the relative spawning stock size from different reefs. Of the

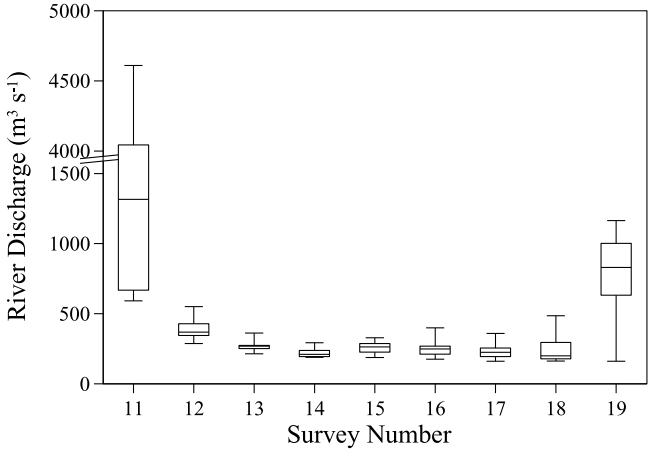

Figure 3. Box plot for daily river discharge during the larval period of surveys 11 to 19. The two end whiskers indicate the minimum and maximum, and the box is defined by the lower and upper quartiles, with the center line for the median.

total larval mass released in model simulations, 90% were released from CPR and the remaining 10% were released from the other unproductive oyster reefs in proportion to their surface area: 4.3% from WHR, 3.4% from PCR, and 2.3% from the reefs in Bon Secour Bay including BSR, SBR, and FRR.

2.3.2.2. Larval Period

[29] The larval period of oysters is affected by various factors such as water temperature, salinity, food availability, and turbidity [*Dekshenieks et al.*, 1993; *Kennedy*, 1996; *Shumway*, 1996]. *Kennedy* [1996, Table 8] reviewed the estimated larval period of eastern oyster as a function of water temperature and showed a negative relationship between larval period and water temperature. Larval period varied from 20 to 30 days at Prince Edward Island, Canada, for water temperature between 18° and 22°C and from 10 to 19 days in other areas for water temperature between 20° and 30°C. The minimum larval period of 10 days was observed for a water temperature of 30°C.

[30] In the present study, larval period was estimated by employing a linear regression between $\ln(T_{\text{larvae}})$ and water temperature based on the oyster data of *Kennedy* [1996, Table 8].

$$T_{\text{larvae}} = 110.76 \times \exp(-0.0825 T_w), \tag{5}$$

where T_{larvae} is the larval period (days) and T_w is the water temperature (°C). The regression shows a significant relationship ($R^2 = 0.57$, $p < 0.001$; $n = 23$) between T_{larvae} and water temperature. For each of surveys 11 to 19 the average bottom water temperature was calculated over the time period since the previous survey (Table 1), using hourly data from the Dauphin Island Sea Lab (DISL) station (Figure 1), maintained by Mobile Bay National Estuary Program. The corresponding larval period was estimated using equation (5) and the minimum observed larval period of 10 days was specified. The estimated larval periods ranged between 10 and 18 days in the Mobile Bay system when the average water temperature varied between 22.0° and 31.2°C (Table 1). The estimates are comparable with those of *Saoud et al.* [2000]: 10 days in August 1999 and 18 days in September 1998.

2.3.2.3. Spawning Time

[31] Among various stimuli initiating spawning events of bivalves, several studies have stressed the importance of water temperature cue to stimulate spawning time of oysters [*Nelson*, 1928; *Hayes and Menzel*, 1981; *Kennedy*, 1996; *Shumway*, 1996; *Thompson et al.*, 1996; *Saoud et al.*, 2000]. Increases in water temperature to a critical threshold of 20°C initiated mass spring spawning in estuaries in New Jersey, and increases to 25°C did so in the northeastern Gulf of Mexico [*Nelson*, 1928; *Hayes and Menzel*, 1981]. Summer spawning was stimulated by rapid increases in water temperature by 2°C in Barnegat Bay, New Jersey [*Nelson*, 1928], and by 5°–10°C increases in Turkey Point and Alligator Harbor, Florida [*Hayes and Menzel*, 1981]. Widespread fall spawning was attributable to rapid decreases in water temperature in the northern Gulf of Mexico. For example, rapid decreases in water temperature by 3°–7°C initiated fall spawning of oysters in Fish River Reef in Mobile Bay, Alabama [*Saoud et al.*, 2000]. *Hayes and Menzel* [1981] argued that fall spawning caused by rapid decreases in water temperature may occur in the Gulf of Mexico as early as late July to early August.

[32] In the present study hourly bottom water temperature data at the DISL station were used to determine potential spawning events of oysters. An increase in water temperature to a critical threshold of 25°C, which initiated spring spawning in the northeastern Gulf of Mexico [*Hayes and Menzel*, 1981], was applied to detect initial spring spawning for survey 11. A rapid increase or decrease in water temperature by 2°C or more was applied to detect the summer and fall spawning events for survey 12 to 19. A single spawning event was assumed for each survey, and the estimated times of spawning events are reported in Table 1. Because more than one spawning event was possible from the temperature cues for some surveys, model sensitivity was examined for alternate spawning times.

2.4. Model Validation

[33] The larval transport model was run for 215 days between 1 April and 1 November 2006. For each survey larvae were released instantaneously at the estimated spawning time (Table 1) and simultaneously from the bottom layer at all spawning locations (Figure 1). Larvae were transported over the estimated larval period until the starting day of each survey, and then a tidal cycle, 25 h, average larval concentration was calculated in the bottom layer and compared with the data. Model-data comparisons were conducted at three time scales of overall average, season, and survey.

[34] For a quantitative model-data comparison, zone-based spatial aggregation was conducted; the median of the data and the model results were calculated for each of the five zones, EMS, CP, LMB, MMB, and BSB (Figure 1). The zone-median data showed an overall pattern consistent with the original data for both oyster spat settlement and bivalve larval concentration. To facilitate direct comparison, the zone-median model results were normalized by the median oyster spat settlement and bivalve larval concentration in EMS over nine surveys:

$$C_{M,\text{spat}}(i,j) = \frac{C_M(i,j) \times C_{\text{spat}}(\text{EMS, median})}{C_M(\text{EMS, median})}, \tag{6}$$

$$C_{M,\text{larvae}}(i,j) = \frac{C_M(i,j) \times C_{\text{larvae}}(\text{EMS, median})}{C_M(\text{EMS, median})}, \tag{7}$$

where $C_M(i,j)$ are the model results in the ith zone for the jth survey; $C_{M,\text{spat}}$ and $C_{M,\text{larvae}}$ are the normalized model results in units of spats (spats m^{-2} d^{-1}) and bivalve larval concentration (larvae per 10 L), respectively; C_M(EMS, median) is the median model result in EMS over nine surveys; C_{spat}(EMS,median) and C_{larvae} (EMS,median) are the median spat settlement and larval concentration, respectively, in EMS over nine surveys. Then, correlation analyses were conducted to compare the normalized model results with both types of data.

3. Results

3.1. Field Data

3.1.1. Water Column Stratification

[35] Water column stratification may play an essential role in larval transport in an estuarine system. Stratification

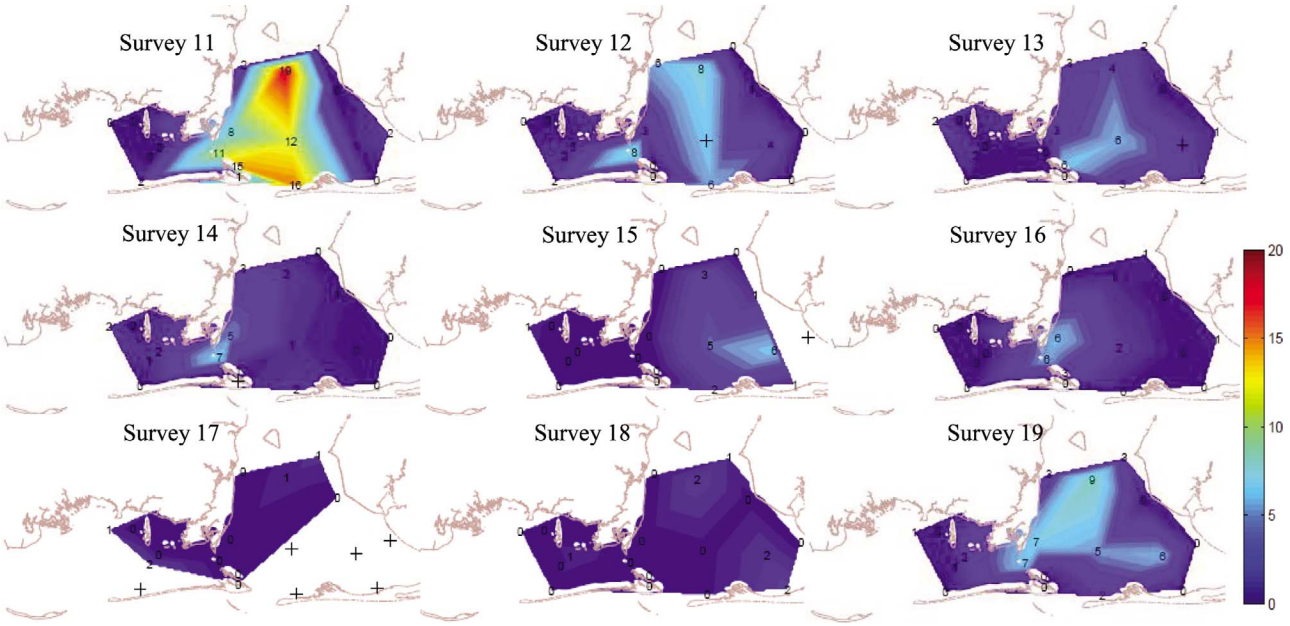

Figure 4. Observed bottom-surface salinity difference (psu) in surveys 11 to 19; crosses indicate missing data. Surface and bottom salinity was measured at 0.5 m from the surface and bottom, respectively, except at stations near the ship channel, where salinity at a 3 m depth was used for bottom salinity.

controls vertical mixing, which in turn affects the vertical distribution of planktonic larvae and thus may change their net horizontal transport [*Kennedy*, 1996; *Shen et al.*, 1999; *Pringle and Franks*, 2001]. The CTD casting data in 2006 showed that the bottom-surface density difference was mostly determined by the corresponding salinity difference ($R^2 > 0.99$, $p < 0.001$; $n = 152$), and thus stratification was described in terms of salinity difference.

[36] Spatial heterogeneity in water column stratification was apparent in the Mobile Bay system (Figure 4). The bottom-surface salinity difference in EMS was less than 2 psu for all nine surveys. A large salinity difference, over 5 psu, was observed in EMS only during the surveys conducted in February–March 2006, when the median river discharge was greater than 2000 $m^3\ s^{-1}$ (not shown). In CP the bottom-surface salinity difference showed different responses to tidal and wind forcing depending on river discharge. When river discharge was less than 500 $m^3\ s^{-1}$, a large salinity difference developed in CP during equatorial tide with calm winds, for example, surveys 14 and 16, and the large gradient disappeared during tropic tide or strong wind conditions, for example, surveys 13, 15, 17, and 18. When river discharge was relatively high during surveys 11 and 19, in contrast, a large salinity difference, over 5 psu, developed in CP even under tropic tide and strong wind conditions. A large bottom-surface salinity difference, over

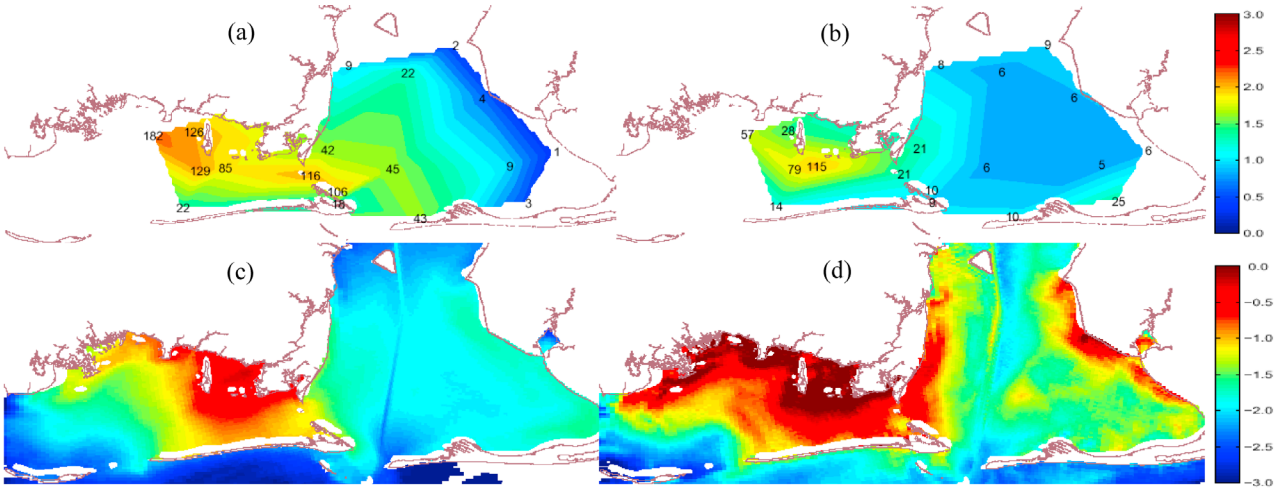

Figure 5. Observed (a) oyster spat settlement (spats $m^{-2}\ d^{-1}$) and (b) bivalve larval concentration (larvae per 10 L) compared with the model results (c) by physical transport only and (d) by physical transport and biological movement, averaged over surveys 11 to 19. Color bars indicate $\log_{10}$-transformed data and model results.

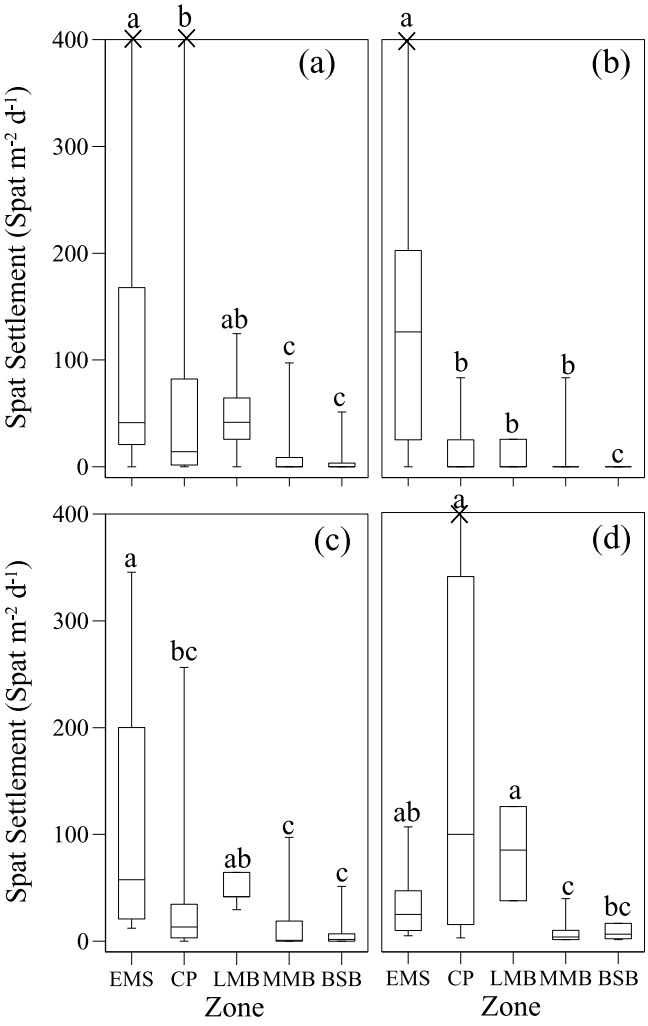

Figure 6. Box plot for the observed oyster spat settlement in five zones (a) for all surveys (surveys 11–19) and for seasons of (b) spring (surveys 11–13), (c) summer (surveys 14–16), and (d) fall (surveys 17–19). The two end whiskers indicate the minimum and maximum, and the box is defined by the lower and upper quartiles, with the center line for the median. Data larger than 400 spats m^{-2} d^{-1} are marked with a cross at the top of the plots. Different lowercase letters (i.e., a, b, and c) above the upper whiskers indicate a significant difference ($p < 0.05$) between zones.

5 psu, was observed in the upper 3 m water column near the ship channel: see surveys 11–13, 15, and 19. The salinity difference was always less than 2 psu in the shallow stations in BSB, but a large salinity difference was observed in the center of BSB during surveys 15 and 19, when the upper 3 m water column was strongly stratified along the ship channel.

3.1.2. Oyster Spat Settlement and Bivalve Larval Concentration

[37] Spat settlement of oysters averaged over surveys 11 through 19 showed a gradient decreasing from west to east (Figure 5a), consistent with previous observations [*Hoese et al.*, 1972; *Lee*, 1979; *Saoud et al.*, 2000]. The maximum settlement was observed in EMS, which was significantly higher than the second peak in CP, while MMB and BSB showed significantly lower settlement (Figure 6a). Seasonal variations were apparent in oyster spat settlement. EMS showed bimodal peaks in spring and summer, whereas CP had a single peak in fall. These peak settlements in EMS and CP were significantly higher than those in MMB and BSB. The distribution of oyster spat settlement showed a gradient decreasing from west to east in eight of nine surveys (Figure 7). The only exception was survey 14, when the maximum, yet relatively weak, spat settlement occurred along the ship channel in Mobile Bay.

[38] The larval concentration of bivalves averaged over surveys 11 through 19 also showed a gradient decreasing from west to east (Figure 5b). The maximum larval concentration was observed in EMS, which, unlike spat settlement, was not significantly higher than that in CP, and larval concentrations in LMB, MMB, and BSB were significantly lower than that in EMS (Figure 8a). Seasonal variations were also apparent in bivalve larval concentration. In spring the peak larval concentration occurred in EMS, which was significantly higher than that in MMB and BSB. In summer, unlike oyster spat settlement, the peak larval concentration occurred in BSB but the larval concentration was not significantly different between zones. In fall the maximum median larval concentration occurred in EMS and the second peak occurred in CP, but they were not significantly different. The distribution of bivalve larval concentration showed a gradient decreasing from west to east in eight of nine surveys (Figure 9). The only exception was survey 15, when the maximum larval concentration occurred in BSB. Note that the data from survey 12 show a quite low larval concentration throughout the study area, resulting in a weak gradient decreasing from west to east.

[39] Oyster spat settlement and bivalve larval concentration from all surveys were significantly correlated ($R = 0.50$) (Table 2), and both data, averaged over the nine surveys, exhibited a west-east gradient, with maximum abundance in the southwestern part of the Mobile Bay system (Figure 5). In seasonal comparisons a significant correlation between oyster spat settlement and bivalve larval concentration existed only in spring ($R = 0.69$) (Table 2). In particular, they showed the highest correlation in May (survey 11; $R = 0.76$, $n = 17$) and June (survey 13; $R = 0.68$, $n = 15$). No significant correlation existed between the two types of data in summer and fall (Table 2). In summer, oyster spat settlement showed the maximum peak in EMS (Figure 6c), while the maximum peak in bivalve larval concentration was in BSB (Figure 8c). In fall the maximum oyster spat settlement occurred in CP (Figure 6d), with four times higher settlement in surveys 18 and 19 than in survey 17 (Figure 7). In contrast, the maximum bivalve larval concentration occurred in CP for survey 17 only and in EMS for surveys 18 and 19 (Figure 9). Despite these relatively small-scale differences, a gradient decreasing from west to east persisted in both data in seven of nine surveys, all but surveys 14 and 15.

3.2. Model-Data Comparison

3.2.1. Physical Transport

[40] The model results by physical transport only (i.e., $w_{bi} = 0$ in equation (1)), averaged over surveys 11 to 19 (Figure 5c), showed good agreement with both oyster spat settlement and bivalve larval concentration. The maximum

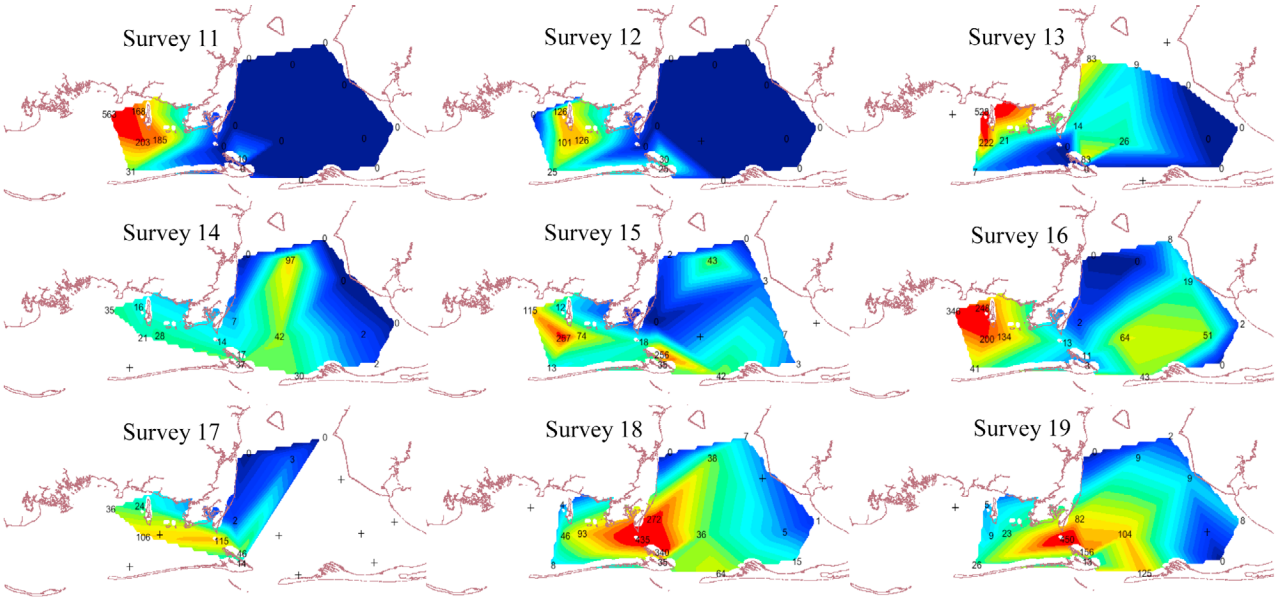

Figure 7. Observed oyster spat settlement (spats m^{-2} d^{-1}) in surveys 11 to 19. The color contour is based on the color bar in Figure 5 and crosses indicate missing data.

model results appeared in the northern part of EMS and CP, while concentrations in the middle and east sides of the bay were much lower, consistent with the observations. The normalized model results were significantly correlated with both spat settlement ($R = 0.47$) and larval concentration ($R = 0.57$) (Table 2). The model results agreed with the observed spat settlement in that both showed maximum medians in EMS and maximum variations in CP (Figure 10a). Both the model results and the bivalve larval concentration showed maximum medians in EMS, but the modeled maximum variation occurred in CP, whereas the observed maximum variation occurred in EMS (Figure 10b).

[41] The model results showed a consistent pattern for all three seasons (not shown): model results in the southwest part an order of magnitude higher than those in the middle and east sides of the bay. When oyster spat settlement and bivalve larval concentration showed the strongest correlation in spring ($R = 0.69$), the model results were mostly correlated with both types of data, with Rs of 0.62 and 0.69 for spat settlement and larval concentration, respectively (Table 2). No significant correlation existed between model and either type of data in summer when neither type of data showed a significant correlation. Both data showed no significant correlation in fall, and the model results were significantly correlated with larval concentration only.

[42] The model results by physical transport only consistently showed the typical gradient, decreasing from west to east, for each of surveys 11 to 19 (Figure 11). The model results were in good agreement with oyster spat settlement and bivalve larval concentration whenever the west-east gradient was present in the data. The west-east gradient was more persistent in model results than in data, such that the model could not reproduce the exceptional patterns observed in survey 14 for spat settlement or in survey 15 for larval concentration.

3.2.2. Biological Movement

[43] Figure 5d shows the model results by the combined effects of physical transport and biological movement averaged over surveys 11 to 19. The gradient decreasing from west to east was still apparent, with the peak concentration again occurring in the northern part of EMS and CP. Compared to the model results by physical transport only (Figure 5c), biological movement increased larval retention, especially in the southwest part of the study area and along the western and eastern shores of Mobile Bay (Figure 5d). In addition, it enhanced the patchiness in distribution, with small patches with a high concentration appearing in most zones, even in the east side of the bay. The normalized model results were significantly correlated with both oyster spat settlement ($R = 0.40$) and bivalve larval concentration ($R = 0.62$) (Table 2) and showed a distribution in each zone similar to that by physical transport only (Figure 10).

[44] Inclusion of biological movement did not change seasonal patterns in model results (not shown): higher model results in the southwest part than in the middle and east sides of the bay. As in the case of physical transport only, the normalized model results were significantly correlated with both spat settlement ($R = 0.53$) and larval concentration ($R = 0.71$) in spring (Table 2). In summer no significant correlation existed between model and either type of data. In fall the model results showed a significant correlation with larval concentration but not with spat settlement, as in the case of physical transport only.

[45] Inclusion of biological movement did not change the modeled patterns for each survey, which again consistently showed the typical gradient decreasing from west to east (not shown). As in the case of physical transport only, the west-east gradient was persistent in model results, such that the model could not reproduce the exceptional patterns

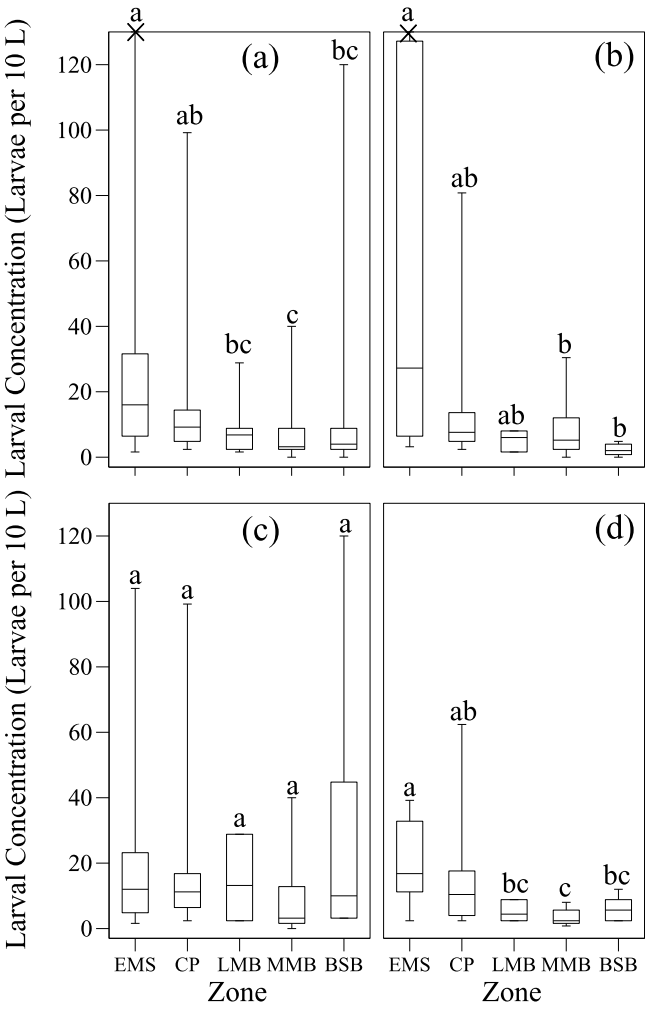

Figure 8. Box plot for the observed bivalve larval concentration in five zones (a) for all surveys (surveys 11–19) and for seasons of (b) spring (surveys 11–13), (c) summer (surveys 14–16), and (d) fall (surveys 17–19). The two end whiskers indicate minimum and maximum, and the box is defined by the lower and upper quartiles with the center line for the median. Data larger than 130 larvae per 10 L are marked with a cross at the top of the plots. Different lowercase letters (i.e., a, b, and c) above the upper whiskers indicate a significant difference ($p < 0.05$) between zones.

observed in survey 14 for spat settlement and in survey 15 for larval concentration.

3.3. Model Sensitivity

[46] For biological movement the present model employs neutrally buoyant early-stage larvae and net sinking late-stage larvae (VM in Figure 2). Inclusion of VM, compared to the case of physical transport only, increased larval retention in all zones, particularly in EMS and CP (Figures 5 and 12). Model sensitivity was examined for two other parameterization methods of biological movement (Figure 2), VM_{swim} (net swimming of early-stage larvae) and VM_{sink} (twice-as-fast net sinking of late-stage larvae). VM_{swim} caused relatively more early-stage larvae to stay in the water column, where they were subject to a stronger current, thus resulting in higher dispersion and decreased larval retention in most zones (Figure 12). VM_{sink}, in contrast, enhanced larval retention owing to increased net sinking velocity of late-stage larvae, particularly in the spawning zone, CP (Figure 12). Despite the differences in larval retention, however, the gradient decreasing from west to east was apparent in model results regardless of the modeling methods of biological movement. The model results with any modeling method of biological movement always showed the peak concentration in EMS and CP at time scales of overall average, season, and survey.

[47] More than one spawning event could have been selected for some surveys based on the criterion of a rapid temperature change over 2°C. Model sensitivity to alternate spawning times was examined. As the spawning time changed for a survey, the larval period, the time period between the spawning time and the time of the survey, also changed. Therefore, model sensitivity to larval period was also examined. Despite the differences in spawning time and larval period by 2–7 days, the model results showed consistent patterns of distribution for each survey (not shown). Because of dilution effects the modeled concentration decreased as the larval period increased, but without changing the overall patterns of distribution, confirming that the model results were not sensitive to spawning time or larval period. The model results were not sensitive to the period of time either, with the average ranging from one to five tidal cycles.

4. Discussion

[48] Production of larvae, larval transport and supply, larval settlement, and postsettlement survival to adults determine recruitment of marine organisms with planktonic larval stages, and variation in each of these components has the potential to regulate their populations [*Kennedy*, 1996; *Underwood and Keough*, 2001]. Among these processes, larval transport plays a critical role in determining spatial and temporal patterns of many marine invertebrates and fish [*Morgan*, 1995; *Kennedy*, 1996]. Therefore, studies of larval transport may provide valuable information for restoration or management of exploited marine populations [*Palumbi*, 2003; *Pineda et al.*, 2007]. Here we conducted a field and modeling study to investigate larval transport of eastern oyster, focusing on the controlling processes responsible for the persistent gradient decreasing from west to east in spat settlement, seasonal variations in larval transport and retention, and relevance of biological movement of larvae in Mobile Bay and eastern Mississippi Sound, Alabama.

[49] As with any numerical modeling study, model validation through model-data comparison is important to ensure model reliability and to evaluate limitations of model applications. We collected two types of field data, oyster spat settlement and bivalve larval concentration, throughout the study area in 2006. Neither, however, is an exact measure of oyster larval concentration, with each having its own positive and negative aspects as a proxy of potential oyster recruitment. Oyster spat settlement is the result of oyster larval supply, modified by settlement and postsettlement processes. If postsettlement mortality is significantly different among stations, the distribution in spat settlement may not properly represent the larval supply of oysters to the

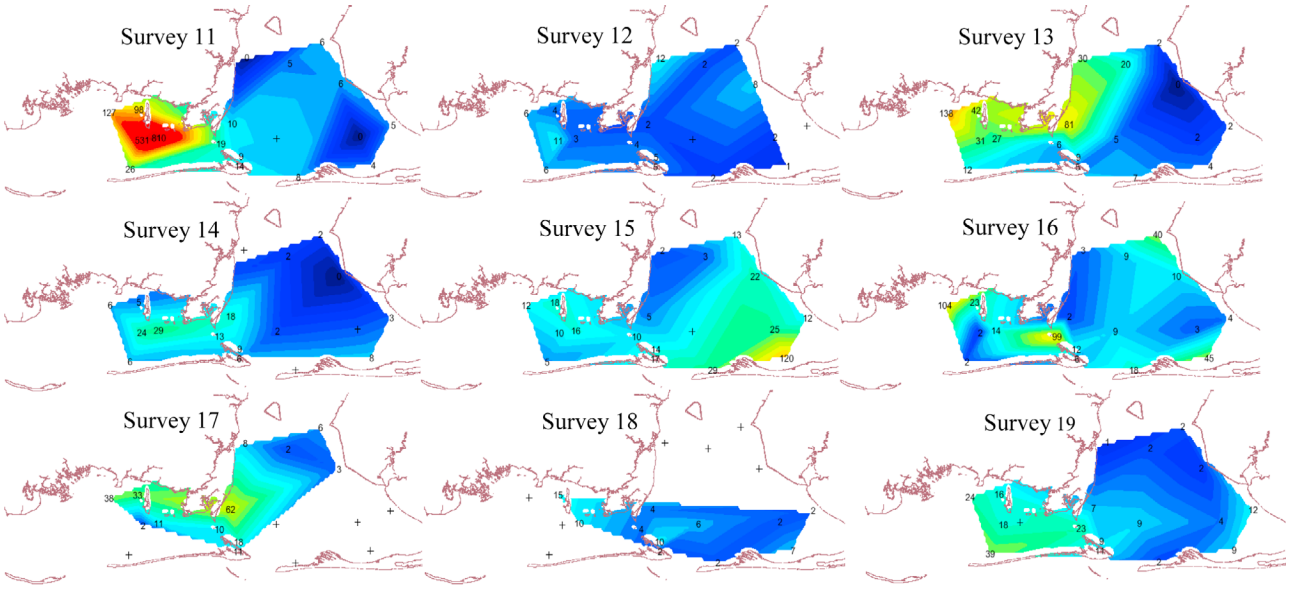

Figure 9. Observed bivalve larval concentration (larvae per 10 L) in surveys 11 to 19. The color contour is based on the color bar in Figure 5 and crosses indicate missing data.

stations. Bivalve larval concentration directly represents larval supply to each station not affected by settlement and postsettlement processes, but it includes larvae of all bivalves. Bivalve larval concentration, therefore, is determined by the most dominant larval organisms at each station during the survey. When both types of data show a consistent pattern, either may be considered a good proxy of oyster larvae.

[50] Both oyster spat settlement and bivalve larval concentration, averaged over the nine surveys, exhibited a gradient decreasing from west to east, with maximum abundance in the southwestern part of the study area (Figure 5). This agreement suggests that both oyster spat settlement and bivalve larval concentration may be good indicators of the overall average patterns of oyster larval supply. Seasonal patterns were apparent in oyster spat settlement (Figure 6) and bivalve larval concentration (Figure 8). Oyster spat settlement showed bimodal peaks in EMS in spring and summer, whereas CP had a single peak in fall, consistent with previous observations [*Hoese et al.*, 1972; *Lee*, 1979; *Saoud*, 2000]. Bivalve larval concentration showed bimodal peaks in EMS in spring and fall. Significant correlation between both types of data existed in spring, suggesting that the maximum spring peak in oyster spat settlement in EMS was likely due to the high larval supply. In summer the maximum peak in bivalve larval concentration in BSB (Figure 8c), with a very low corresponding spat settlement (Figure 6c), seems to be due to bivalves other than oyster larvae. In fall the bivalve larval concentration showed the maximum peak in EMS, while oyster spat settlement did so in CP. Both types of data showed gradients decreasing from west to east in seven of nine surveys, all except surveys 14 and 15.

[51] The model reproduced average patterns of both oyster spat settlement and bivalve larval concentration, showing a consistent west-east gradient (Figure 5). The model showed the best results in spring, when both types of data showed the strongest correlation (Table 2). No significant correlation, however, existed between the model and any of the data in summer, which may be attributable to the occurrence of exceptional patterns in both types of data. In fall the model results were significantly correlated with the bivalve larval concentration, both showing the maximum peak in EMS, but did not reproduce the maximum peak in CP observed in oyster spat settlement. Hence, larval supply alone may not be the controlling process for the observed fall peak settlement of oyster spat in CP. In a survey-by-survey comparison, the model reproduced the observed patterns when both types of data showed a gradient decreasing from west to east, but could not reproduce exceptional patterns (Figures 7, 9, and 11). The model results always showed a peak concentration in EMS and CP at time scales of overall average, season, and each survey, regardless of

Table 2. Correlation Coefficients (R) Among Oyster Spat Settlement, Bivalve Larval Concentration, and Model Result by Physical Transport[a]

Variables	Overall (Surveys 11–19)	Spring (Surveys 11–13)	Summer (Surveys 14–16)	Fall (Surveys 17–19)
Spat settlement vs. larval concentration	0.50*(n = 42)	0.69*(n = 15)	0.49(n = 15)	0.20(n = 12)
Model result vs. spat settlement	0.47*(0.40*)(n = 43)	0.62*(0.53*)(n = 15)	0.47(0.41)(n = 15)	0.35(0.26)(n = 13)
Model result vs. larval concentration	0.57*(0.62*)(n = 42)	0.69*(0.71*)(n = 15)	0.39(0.37)(n = 15)	0.62*(0.82*)(n = 12)

[a]Values in parentheses indicate correlation coefficients with the model result by the combined effects of physical transport and biological movement. Both zone-median data and normalized model results (equations (6) and (7)) were $\log_{10}$ transformed before correlation analysis. *Significant relationship at $p < 0.05$.

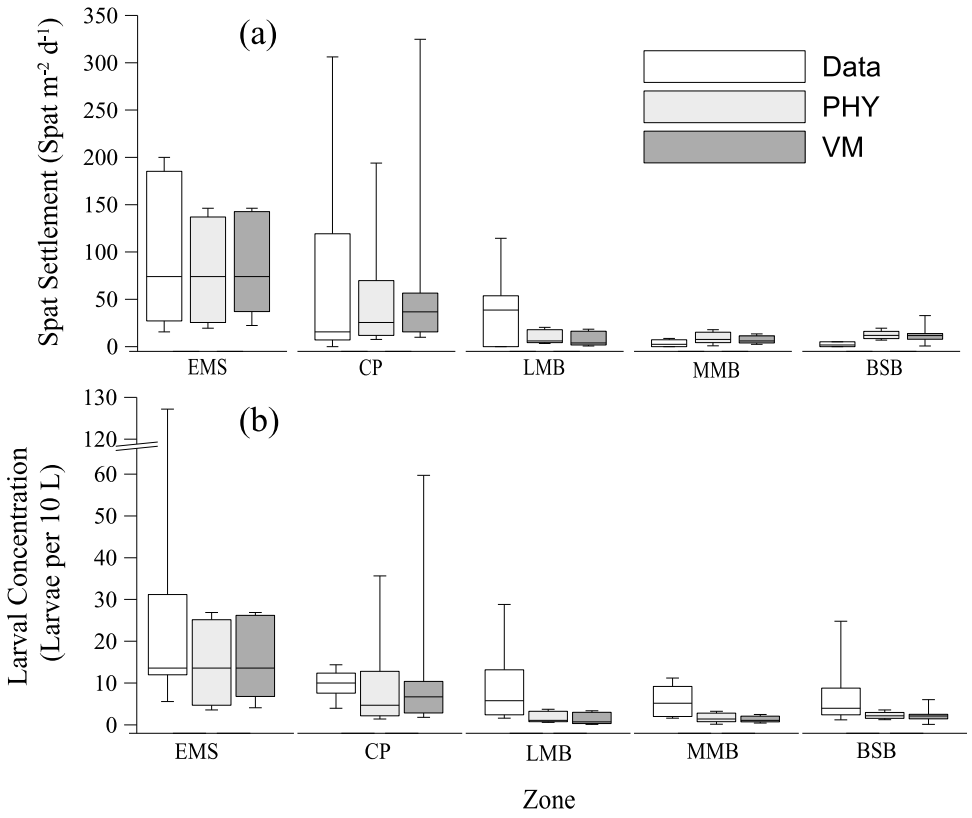

Figure 10. Model-data comparison for (a) oyster spat settlement and (b) bivalve larval concentration. Model results for physical transport only (PHY) and for physical transport and biological movement (VM) were normalized using equations (6) and (7). The two end whiskers indicate the minimum and maximum, and the box is defined by the lower and upper quartiles, with the center line for the median.

forcing conditions. Such a persistent gradient decreasing from west to east in the model results suggests that larval supply may be a controlling process for the corresponding gradient in oyster spat settlement observed over the past 40 years.

[52] Observations indicated that biological movement may enhance larval retention within estuarine systems [*Carriker*, 1951; *Andrews*, 1983; *Kennedy*, 1996; *Rose et al.*, 2006]. *Rose et al.* [2006] suggested that behavioral adjustment may be the mechanism allowing local recruitment of oysters in outflux dominant estuarine systems. The present model application showed similar results in that biological movement of oyster larvae enhanced their retention within the study area (Figures 5d and 12). Net sinking of late-stage

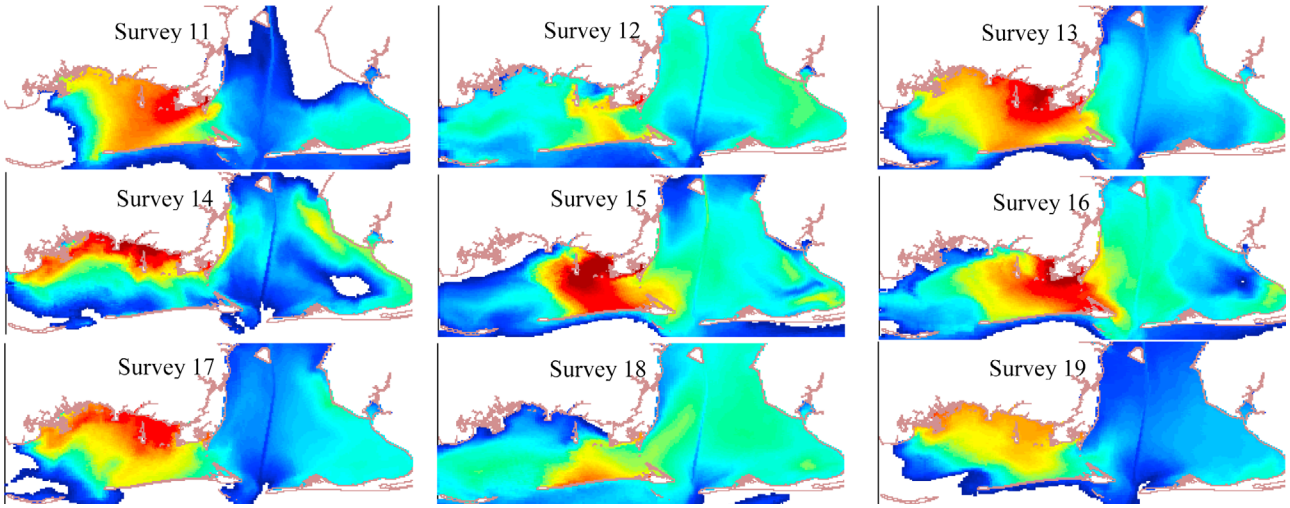

Figure 11. Model results by physical transport only for surveys 11 to 19. The color contour is based on the color bar in Figure 5.

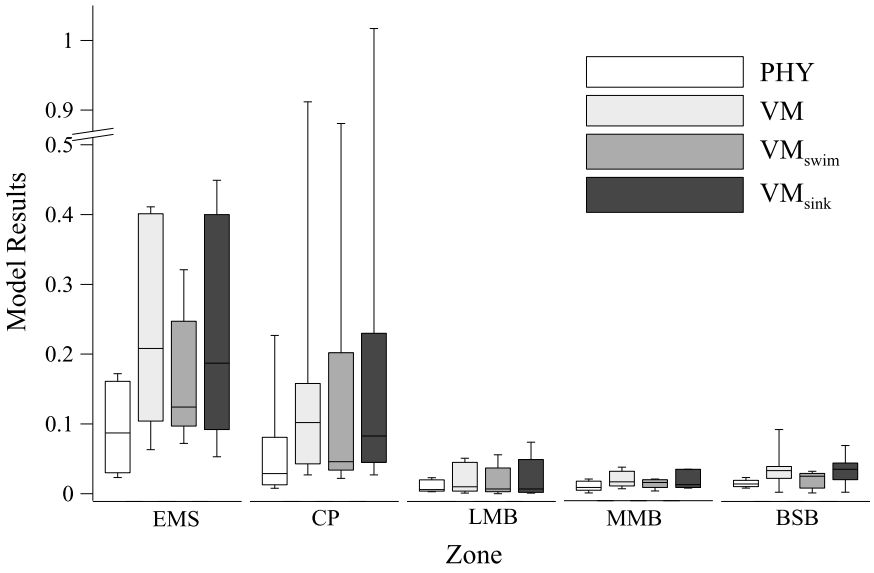

Figure 12. Comparison between the model results by physical transport only (PHY) and those with biological movement, including neutral buoyancy at the early stage and net sinking at the late stage (VM), net swimming at the early stage and net sinking at the late stage (VM_{swim}), and neutral buoyancy at the early stage and twice-as-fast net sinking at the late stage (VM_{sink}). The two end whiskers indicate the minimum and maximum, and the box is defined by the lower and upper quartiles, with the center line for the median.

larvae enhanced larval retention mainly in the southwestern part of the study area. Increases in net sinking velocity of late-stage larvae resulted in the largest increase in larval retention in CP, the spawning zone, which provides a favorable conditions for local recruitment of oysters. Biological movement also enhanced the patchiness in larval distribution (Figure 5d), consistent with the observations that late-stage oyster larvae exhibited pronounced patchiness in estuarine systems [*Kennedy*, 1996]. *Franks* [1992] suggested that the combined effects of behavioral larval movement and flow patterns may determine the horizontal and vertical scales of patchiness.

[53] In the Mobile Bay system, inclusion of biological movement resulted in little change in the overall patterns of oyster larval transport, resulting in a consistent west-east gradient compared to physical transport only. This may be attributable to frequent destratification in the southwestern part of the study area, EMS and CP, during larval recruitment periods in May–October, with seasonally low river discharge (Figure 3). The CTD casting data from nine surveys in 2006 showed a destratified water column, with the bottom-surface salinity difference less than 2 psu in EMS (Figure 4). In CP, five of nine surveys showed highly stratified conditions, with the bottom-surface salinity difference larger than 5 psu, but such strong stratification was readily destroyed during tropic tide or strong wind conditions when river discharge was less than 500 $m^3\ s^{-1}$. *Schroeder et al.* [1990] suggested that a current speed of 15 cm s^{-1} and a wind speed of 5 m s^{-1} are strong enough to mix a water column associated with a river discharge of 500 $m^3\ s^{-1}$. The present model results also showed frequent destratification of the water column in the southwest part of the study area. Such frequent destratification may prevent oyster larvae from utilizing horizontal transport by changing vertical position in the water column. As such, biological movement induced little change in the larval distribution due to physical transport in the Mobile Bay system and likely in other shallow estuarine systems experiencing frequent destratification.

[54] Oyster spat settlement and bivalve larval concentration are influenced by many biological conditions such as variations in spawning time, growth rate, and mortality of larvae and spat, as well as physical transport. *Saoud et al.* [2000] attributed the variability in spat settlement in Mobile Bay to different spawning times in each habitat. *Kennedy* [1996] reviewed that variations in transport patterns, salinity, DO, physiological tolerance, presence of competition and predators, and larval abundance may result in dramatic changes in settlement intensity within a small spatial and short time scale. The present model employed rather simplified biological conditions, with the assumptions of a single spawning event for each type of survey data, a constant linear growth rate, and no mortality of oyster larvae. Such simplifications may be responsible for the model results being less dynamic than the data. The model, nonetheless, gave a good overall description of the observed patterns of oyster spat settlement and bivalve larval concentration in the Mobile Bay system. This model application has been used to establish spatially explicit management strategies for oyster restoration in the Mobile Bay system [*Kim*, 2009]. The current field and modeling approach may be applicable for the study of recruitment of other marine invertebrates and fish, which may provide valuable information for management of exploited marine populations.

5. Conclusions

[55] We developed a larval transport model that accounts for physical transport, biological movement of larvae, and

site- and larval-specific conditions of eastern oysters. We validated the model with field data for oyster spat settlement and bivalve larval concentration collected throughout the Mobile Bay system in 2006. The model reproduced the dominant patterns of both types of data well, showing a consistent gradient decreasing from west to east. The model results always showed a peak concentration in the southwest part of the Mobile Bay system at time scales of overall average, season, and each survey. The persistent west-east gradient in the model results suggests that the larval supply may be responsible for the corresponding gradient in oyster spat settlement observed over the past 40 years. Net sinking of late-stage larvae increased larval retention near the spawning area, thus providing a favorable condition for local recruitment of oysters. Inclusion of biological movement, however, caused little change in the overall patterns of oyster larval transport resulting in a west-east gradient, which may be attributable to frequent destratification in the southwest part of the study area during the oyster larval recruitment period. The model results were not sensitive to model parameters such as spawning time, larval period, and parameterization of biological movement. This study enhances our understanding of the controlling processes for larval transport and retention of oysters in broad, shallow estuarine systems.

[56] **Acknowledgments.** We appreciate the anonymous reviewers' comments, which contributed greatly to the improvement of this paper. We would like to thank Drs. Richard A. Luettich and William W. Schroeder for their constructive comments and guidance throughout this study. We also thank Jason Herrmann, Mairi Miller, Zeb Schobernd, Crystal LouAllen, and Ben LaCour for their help with the field- and laboratory work. This study was funded by the National Marine Fisheries Service, NOAA, via a grant from the University of South Alabama's Alabama Oyster Reef Restoration Program.

References

Andrews, J. D. (1983), Transport of bivalve larvae in James River, Virginia, *J. Shellfish Res.*, *3*(1), 29–40.

Baker, P., and R. Mann (2003), Late stage bivalve larvae in a well-mixed estuary are not inert particles, *Estuaries*, *26*(4A), 837–845.

Bell, J. O. (1952), A study of oyster production in Alabama waters, M.S. thesis, Texas A&M, College Station.

Burrell, V. G., Jr. (1986), Species profiles: Life histories and environmental requirements of coastal fishes and invertebrates (South Atlantic)—American oyster, U.S. Fish and Wildlife Service Biological Report 82(11.57), TR EL-82-4, U.S. Army Corps of Engineers, Slidell, La.

Carriker, M. R. (1951), Ecological observations on the distribution of oyster larvae in New Jersey estuaries, *Ecol. Monogr.*, *21*(1), 19–38.

Carriker, M. R. (1996), The shell and ligament, in *The Eastern Oyster: Crassostrea virginica*, edited by V. S. Kennedy, R. I. E. Newell and A. F. Eble, pp. 75–168, Maryland Sea Grant College, College Park.

Dekshenieks, M. M., E. E. Hofmann, and E. N. Powell (1993), Environmental effects on the growth and development of eastern oyster, *Crassostrea virginica* (Gmelin, 1971), larvae: A modeling study, *J. Shellfish Res.*, *12*(2), 241–254.

Dekshenieks, M. M., E. E. Hofmann, J. M. Klinck, and E. N. Powell (1996), Modeling the vertical distribution of oyster larvae in response to environmental conditions, *Mar. Ecol. Prog. Ser.*, *136*, 97–110.

Dekshenieks, M. M., E. E. Hofmann, J. M. Klinck, and E. N. Powell (1997), A modeling study of the effects of size- and depth-dependent predation on larval survival, *J. Plankton Res.*, *19*(11), 1583–1598.

Franks, P. J. S. (1992), Sink or swim: Accumulation of biomass at fronts, *Mar. Ecol. Prog. Ser.*, *82*(1), 1–12.

Galperin, B., L. H. Kantha, S. Hassid, and A. Rosati (1988), A quasi-equilibrium turbulent energy model for geophysical flows, *J. Atmos. Sci.*, *45*, 55–62.

Galtsoff, P. S. (1964), The American oyster, *Crassostrea virginica* Gmelin, *Fish. Bull.*, *64*, 355–380.

Hamrick, J. M. (1992), *A Three-Dimensional Environmental Fluid Dynamics Computer Code: Theoretical and Computational Aspects*, Virginia Institute of Marine Science, College of William and Mary, Gloucester Point.

Hamrick, J. M. (1996), *User's Manual for the Environmental Fluid Dynamics Computer Code*, Virginia Institute of Marine Science, College of William and Mary, Gloucester Point.

Hayes, P. F., and R. W. Menzel (1981), The reproductive cycle of early setting *Crassostrea virginica* (Gmelin) in the northern Gulf of Mexico, and its implications for population recruitment, *Biol. Bull.*, *160*(1), 80–88.

Hidu, H., and H. H. Haskin (1978), Swimming speeds of oyster larvae *Crassostrea virginica* in different salinities and temperatures, *Estuaries*, *1*(4), 252–255.

Hoese, H. D., W. R. Nelson, and H. Beckert (1972), Seasonal and spatial setting of fouling organisms in Mobile Bay and eastern Mississippi Sound, Alabama, *Ala. Mar. Res. Bull.*, *8*, 9–17.

Ji, Z.-G., M. R. Morton, and J. M. Hamrick (2001), Wetting and drying simulation of estuarine processes, *Estuar. Coast. Shelf Sci.*, *53*, 683–700.

Jonsson, P. R., C. Andre, and M. Lindegarth (1991), Swimming behaviour of marine bivalve larvae in a flume boundary-layer flow: Evidence for near-bottom confinement, *Mar. Ecol. Prog. Ser.*, *79*, 67–76.

Kennedy, V. S. (1996), Biology of larvae and spat, in *The Eastern Oyster: Crassostrea virginica*, edited by V. S. Kennedy, R. I. E. Newell and A. F. Eble, pp. 371–421, Maryland Sea Grant College, College Park.

Kim, C.-K. (2009), A modeling study of oyster larval transport in Mobile Bay and eastern Mississippi Sound, Alabama, Ph.D. thesis, University of South Alabama, Mobile.

Korringa, P. (1952), Recent advances in oyster biology, *Q. Rev. Biol.*, *27*(3), 266–308.

Lee, C. (1979), The seasonal and spatial setting of oyster spat and other setting organisms in Mobile Bay in relation to temperature, salinity, and secchi disc visibility, M.S. thesis, University of Alabama, Tuscaloosa.

Lin, J., and A. Y. Kuo (2003), A model study of turbidity maxima in the York River estuary, Virginia, *Estuaries*, *26*, 1269–1280.

Mann, R. (1988), Distribution of bivalve larvae at a frontal system in the James River, Virginia, *Mar. Ecol. Prog. Ser.*, *50*, 29–44.

Mann, R., and J. S. Rainer (1990), Effect of decreasing oxygen tension on swimming rate of *Crassostrea virginica* (Gmelin, 1971) larvae, *J. Shellfish Res.*, *9*(2), 323–327.

Mann, R., B. M. Campos, and M. W. Luckenbach (1991), Swimming rate and responses of larvae of three mactrid bivalves to salinity discontinuities, *Mar. Ecol. Prog. Ser.*, *68*, 257–269.

May, E. B. (1971), A survey of the oyster and oyster shell resources of Alabama, *Ala. Mar. Res. Bull.*, *4*, 1–53.

Mellor, G. L., and T. Yamada (1982), Development of a turbulence closure model for geophysical fluid problems, *Rev. Geophys. Space Phys.*, *20*(4), 851–875, doi:10.1029/RG020i004p00851.

Moore, H. F. (1913), Condition and extent of the natural oyster beds and barren bottoms of Mississippi Sound, Alabama, Department of Commerce and Labor, Washington, D. C.

Morgan, S. G. (1995), Life and death in the plankton: Larval mortality and adaptation, in *Ecology of Marine Invertebrate Larvae*, edited by L. R. McEdward, pp. 279–322, CRC Press, Boca Raton, Fla.

Morgan, S. G., R. K. Zimmer-Faust, K. L. Heck Jr., and L. D. Coen (1996), Population regulation of blue crabs *Callinectes sapidus* in the northern Gulf of Mexico: postlarval supply, *Mar. Ecol. Prog. Ser.*, *133*, 73–88.

Nelson, T. C. (1928), Relation of spawning of the oyster to temperature, *Ecology*, *9*(2), 145–154.

Noble, M. A., W. W. Schroeder, W. J. Wiseman Jr., H. F. Ryan, and G. Gelfenbaum (1996), Subtial circulation patterns in a shallow, highly stratified estuary: Mobile Bay, Alabama, *J. Geophys. Res.*, *101*(C11), 25,689–25,703, doi:10.1029/96JC02506.

North, E. W., Z. Schlag, R. R. Hood, M. Li, L. Zhong, T. Gross, and V. S. Kennedy (2008), Vertical swimming behavior influences the dispersal of simulated oyster larvae in a coupled particle-tracking and hydrodynamic model of Chesapeake Bay, *Mar. Ecol. Prog. Ser.*, *359*, 99–115.

Palumbi, S. R. (2003), Population genetics, demographic connectivity, and the design of marine reserves, *Ecol. Appl.*, *13*(1), S146–S158.

Perry, H. M., D. R. Johnson, K. Larsen, C. Trigg, and F. Vukovich (2003), Blue crab larval dispersion and retention in the Mississippi Bight: Testing the hypothesis, *Bull. Mar. Sci.*, *72*(2), 331–346.

Pineda, J., J. A. Hare, and S. Sponaugle (2007), Larval transport and dispersal in the coastal ocean and consequences for population connectivity, *Oceanography*, *20*(3), 22–39.

Pringle, J. M., and P. J. S. Franks (2001), Asymmetric mixing transport: A horizontal transport mechanism for sinking plankton and sediment in tidal flows, *Limnol. Oceanogr.*, *46*(2), 381–391.

Rabalais, N. N., F. R. Burditt Jr., L. D. Coen, B. E. Cole, C. Eleuterius, K. L. Heck Jr., T. A. McTigue, S. G. Morgan, H. M. Perry, F. M. Truesdale,

R. K. Zimmer-Faust, and R. J. Zimmerman (1995), Settlement of *Callinectes sapidus* megalopae on artificial collectors in four Gulf of Mexico estuaries, *Bull. Mar. Sci.*, *57*(3), 855–876.

Rose, C. G., K. T. Paynter, and M. P. Hare (2006), Isolation by distance in the eastern oyster, *Crassostrea virginica*, in Chesapeake Bay, *J. Hered.*, *97*(2), 158–170.

Rothlisberg, P. C., J. A. Church, and A. M. G. Forbes (1983), Modelling the advection of vertically migrating shrimp larvae, *J. Mar. Res.*, *41*, 511–538.

Ryan, H. F., M. A. Noble, E. A. Williams, W. W. Schroeder, J. R. Pennock, and G. Gelfenbaum (1997), Tidal current shear in a broad, shallow, river-dominated estuary, *Cont. Shelf Res.*, *17*(6), 665–688.

Saoud, I. G. (2000), Environmental parameters affecting the restoration of an oyster reef in Mobile Bay, Alabama, Ph.D. thesis, Auburn University, Auburn, Ala.

Saoud, I. G., D. B. Rouse, R. K. Wallace, J. Howe, and B. Page (2000), Oyster *Crassostrea virginica* spat settlement as it relates to the restoration of Fish River Reef in Mobile Bay, Alabama, *J. World Aquacult. Soc.*, *31*(4), 640–650.

Schroeder, W. W., S. P. Dinnel, and W. J. Wiseman Jr. (1990), Salinity stratification in a river-dominated estuary, *Estuaries*, *13*, 145–154.

Shen, J., J. D. Boon, and A. Y. Kuo (1999), A modeling study of a tidal intrusion front and its impact on larval dispersion in the James River estuary, Virginia, *Estuaries*, *22*(3A), 681–692.

Shumway, S. E. (1996), Natural environmental factors, in *The Eastern Oyster: Crassostrea virginica*, edited by V. S. Kennedy, R. I. E. Newell and A. F. Eble, pp. 467–513, Maryland Sea Grant College, College Park.

Smith, L. L. (1999), Comparative assessments of three unproductive oyster reefs and a productive reef in Mobile Bay, Alabama, M.S. thesis, Auburn University, Auburn.

Thompson, R. J., R. I. E. Newell, V. S. Kennedy, and R. Mann (1996), Reproductive processes and early development, in *The Eastern Oyster: Crassostrea virginica*, edited by V. S. Kennedy, R. I. E. Newell and A. F. Eble, pp. 335–370, Maryland Sea Grant College, College Park.

Turner, E. J., R. K. Zimmer-Faust, M. A. Palmer, M. Luckenbach, and N. D. Pentcheff (1994), Settlement of oyster (*Crassostrea virginica*) larvae: Effects of water flow and a water-soluble chemical cue, *Limnol. Oceanogr.*, *39*(7), 1579–1593.

Underwood, A. J., and M. J. Keough (2001), Supply-side ecology: the nature and consequences of variations in recruitment of intertidal organisms, in *Marine Community Ecology*, edited by M. D. Bertness, S. D. Gaines and M. E. Hay, pp. 183–200, Sinauer Associates, Inc., Sunderland, Mass.

Wang, W.-X., and Z.-Z. Xu (1997), Larval swimming and postlarval drifting behavior in the infaunal bivalve *Sinonovacula constricta*, *Mar. Ecol. Prog. Ser.*, *148*, 71–81.

Wiseman, W. J., Jr., W. W. Schroeder, and S. P. Dinnel (1988), Shelf-estuarine water exchanges between the Gulf of Mexico and Mobile Bay, Alabama, *Am. Fish. Soc. Symp.*, *3*, 1–8.

Wood, L., and W. J. Hargis Jr. (1971), Transport of bivalve larvae in a tidal estuary, *Eur. Mar. Biol. Symp.*, *4*, 29–44.

Young, C. M. (1995), Behavior and locomotion during the dispersal phase of larval life, in *Ecology of Marine Invertebrate Larvae*, edited by L. R. McEdward, pp. 249–277, CRC Press, Boca Raton, Fla.

Yund, P. O., S. D. Gaines, and M. D. Bertness (1991), Cylindrical tube traps for larval sampling, *Limnol. Oceanogr.*, *36*(6), 1167–1177.

K. M. Bayha, W. M. Graham, K. Park, and S. P. Powers, Department of Marine Sciences, University of South Alabama, Dauphin Island Sea Lab, 101 Bienville Blvd., Dauphin Island, AL 36528, USA.

C.-K. Kim (corresponding author), Department of Biology, Stanford University, 371 Serra Mall, Stanford, CA 94305, USA. (ckim3@stanford.edu)